FLOW VISUALIZATION AND VELOCITY PROFILES FOR GRAINS FLOW AROUND A CYLINDER

By
HABIB M. A. and SHAMS EL-DIN SH.
MECHANICAL POWER ENG. DEPARTMENT, FACULTY OF ENG.
MENOUFIYA UNIVERSITY, SHEBIN EL-KOM, EGYPT.

ABSTRACT:

An experimental investigation of velocity profiles of rice grains flow around a cylinder concerning the effect of layers mean velocity and diameter ratio was carried out. The resulting flow patterns produced with the aid of the black tracer technique was used to determine the flow velocity coefficient distributions for diameter ratio ranges from 0.05 to 0.30. The layers mean velocity was ranged from 2 to 18 mm/sec. Development stages of grains flow patterns around the cylinder which were located in a vertical downward flow were photographed. The variation of the flow velocity coefficient in the upstream and downstream of the cylinder with the diameter ratio and the layers mean velocity were discussed. From the observation of the flow patterns and the determination of the flow velocity coefficients distributions, it is found that the stagnant, attachment and flow separation regions formed around the cylinder play a significant role in determining the flow characteristics around the cylinder and they depend strongly on both the mean velocity and the diameter ratio.

1. INTRODUCTION:

The progress in food products technology field during the past few years has brought some new prospects for better reutilizing thermal energy from residual gases. One of the most efficient units for drying agricultural products is the use of heat pipe-heat exchanger systems [1-5]. The circular cylinder in cross grains flow is the most extensively used element in the structure of these systems. The study of grains flow characteristics over these surfaces is significant in understanding the system performance. These characteristics include: the behavior of grain layers in flows, i.e.; stagnant and attachment regions formation besides the flow separation region. In analyzing these formed regions, knowledge of the

MANUSCRIPT RECEIVED FROM DR: HABIB M. A. AT:16/5/1996, ACCEPTED AT:6/2/1996, PP 1- 22
ENGINEERING RESEARCH BULLETIN,VOL,19,NO. 2, 1996
MENOUFIYA UNIVERSITY, FACULTY OF ENGINEERING,
SHEBINE EL-KOM, EGYPT. ISSN. 1110 - 1180

effect of the layers flow velocity and the cylinder diameter on the flow pattern characteristics is very important. This makes it possible to expect and explain the variation of the heat transfer rates around the cylindrical surface of the system.

Most of the published literature on the flow pattern around the cylindrical surfaces are only applicable to fluid flow. There have been very few investigations devoted to a single cylinder and/or tube banks, heat pipe-heat exchanger, placed transversely in the direction of the grains [4, 5]. Pordo et al. [4] studied the heat transfer rates between the condenser part of the heat pipe and wheat grains in cross flow for both a single tube and a bank of tubes. Attention is directed to the dependence of the heat transfer coefficient on the grain layers mean velocity as well as the cylinder diameter. Their results indicated that the best performance of the drying process occurs when the mean velocity of flowing grains ranges from 2 to 24 mm/sec, when the cylinder diameter ranges from 10 to 40 mm. Experimental work presented in [5] had brought brief study on the thermal characteristics of wheat grains flow over cylindrical surfaces. The limited visual observations performed in this study demonstrate that the grains accumulate on the front part of the cylinder, while flow separation region is occurred at the rear part. Figure 1 illustrates the different regions formed around the cylinder and the flow pattern.

In the present study, the effect of the layers mean velocity and the diameter ratio (cylinder diameter to channel width ratio) on the velocity profiles of rice grains flow around a cylinder have been investigated. The development stages of the flow pattern were first studied photographically. From the observation of the flow patterns and the determination of the flow velocity coefficients distributions, the flow characteristics around the cylinder have been discussed.

2. EXPERIMENTAL APPARATUS AND PROCEDURES:

The experiments were carried out in an apparatus whose test section was consisted of a closed vertical squared channel. Three walls of the channel were made of galvanized iron, while the facing wall was prepared from Plexiglas to permit visual observations and consequently photographing the flow patterns. The essential parts of the apparatus are presented in Fig. 2. An open hopper made of iron was mounted at the top of the test section to feed the grains. The tested cylinder was mounted exactly in the channel center line. The cylinder diameters were chosen in such a way that the channel wall does not affect the flow pattern. Rice grains were used in the present experiments. The density of the grains is 1008 kg/m^3 in which the average grain size and humidity are 20.9 mm^3 and 8 %, respectively [5]. The typical flow field produced by the flowing grain particles around the cylinders was obtained with a black tracer technique by adding a thin layer of black powder to the flow materials in the far upstream of the cylinder.

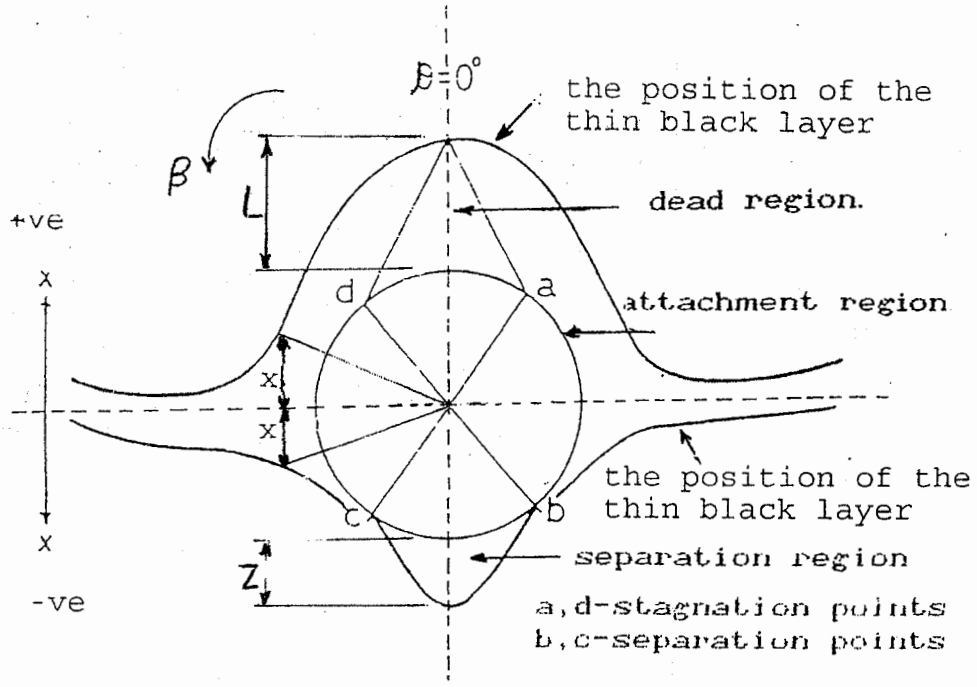

Fig.1 : Flow pattern distribution of grain layers over cylindrical surfaces.

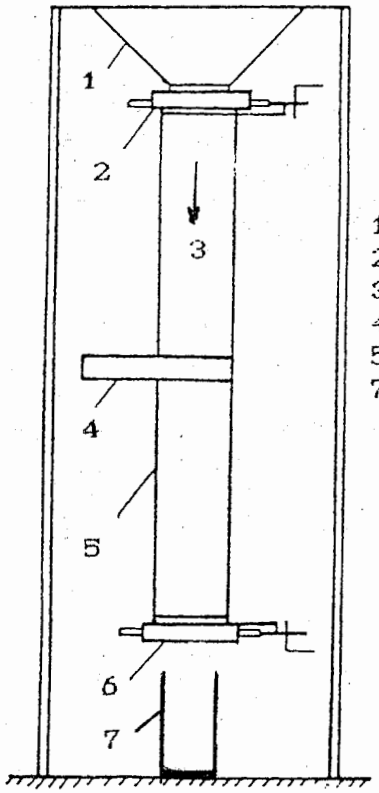

1. -hopper.
2,6. -slide gates.
3. -rice flow direction.
4. -test cylinder
5. -test section.
7. -collector.

Fig.2: Schematic diagram of experimental apparatus.

Flow discharge of the grain particles was controlled by means of a slide gate located at the bottom part of the test section. Another slide gate was located at the upper part to maintain the required discharge from the hopper and to facilitate the addition of the thin black layer to the main flow. Rice grains mean velocity V_m was determined by measuring the time for grains to flow through a certain known distance. The distance was measured from the location of the black thin layer in the far upstream to the horizontal centerline of the cylinder. Grains theoretical velocity (V_{max}) was obtained at the horizontal centerline of the cylinder according to the continuity equation. At this location, V_{max} is given by:

$$V_{max} = V_m . 1/(1-D) \qquad (1)$$

Where V_m is the grains mean velocity, 1 and (1-D) are the total and the free flow widths of the channel.

Two values of grains local velocities were determined. They are: (1) the local mean velocity V_{lm} which is obtained at different locations in the upstream and downstream of the cylinder, and (2): the local values that is obtained around the cylinder V_l. The local mean velocity of grains was determined by applying the continuity equation between two different positions using the measured mean velocity, the channel and the free flow widths. The local velocity distribution around the cylinder was determined from the recorded flow patterns in such a way that the vertical distance (x) was subtracted from the theoretical velocity in the upstream of the cylinder, while it is added in the downstream direction [10]. The error in measuring the particles velocity is less than 3 % depending on the diameter ratio.

In addition, two values of the flow velocity coefficients were determined according to the values of the grains local velocity. These include: (1) the average flow velocity coefficient $\bar{\psi}$ which is obtained at different locations in the upstream and downstream of the cylinder, and: (2) the local flow velocity coefficient ψ that is obtained around the cylinder. The average flow velocity coefficient is considered the relation between the local mean and the theoretical velocities of the grains in the following form:

$$\bar{\psi} = (V_{max} - V_{lm})/V_{max} \qquad (2)$$

Where V_{lm} is the grains local mean velocity at different locations in the upstream and downstream of the cylinder. The local flow velocity coefficient around the cylinder was determined as follows:

$$\psi = (V_{max} - V_l)/V_{max} \qquad (3)$$

Where V_l is the grains local velocity around the cylinder.

The experimental conditions in the present work are tabulated as follows:

Dimensions of grains flow channel	200 x 200 x 1200 mm
Diameter of the test cylinders, D	10, 20, 30, 40, 50 and 60 mm.
Diameter ratio, cylinder diameter to channel width, D/b	0.05, 0.10, 0.15, 0.20, 0.25 and 0.30
Mean velocity in the main flow, V_m	2, 6, 9, 14 and 18 mm/sec.

The procedures using the apparatus shown in Fig. 2 were as follows:

1- At the upstream of 250 mm from the horizontal centerline of the cylinder, the thin black powder was added to the flow materials.

2- When the thin black layer outer edges reaches the horizontal centerline of the cylinder, the lower slide gate was closed and the flow pattern around the cylinder was photographed and recorded using a transparent paper.

3- At the same grain flow rate, a new black layer was added and the grains motion was resumed and step 2 was repeated.

4- The upper slide gate was opened and the flow particles were permitted to fill again the test section.

5- For each experimental run a new black layer was used and the flow pattern was photographed and recorded. The development stages of flow patterns upstream and downstream of the cylinder were also photographed.

3. RESULTS AND DISCUSSIONS:

The results were obtained for rice grains flow around the cylinder for two different parameters that affect the flow pattern. These parameters include: the layers mean velocity and the diameter ratio. The results of the flow visualization and the velocity coefficients are discussed bellow.

3.1. Observation of the Grains Flow Pattern With Photographs:

The black tracer technique was found to be very useful to observe the development of grains flow patterns around the cylinder. In the undisturbed zone, the intergranular friction is very small due to the small relative motion of the grains. In the vicinity of the cylinder the friction between grains and the cylinder is high and this is reflected on the flow pattern. It was very impossible to observe the flow pattern in the inner flow. The photographic view of the flow patterns after adding the thin black layer to the main flow is shown in figures 3-a, b and c. The flow visualization was carried out on diameter ratio (D/b) of 0.30 (D=60 mm) at layers mean velocity of 2

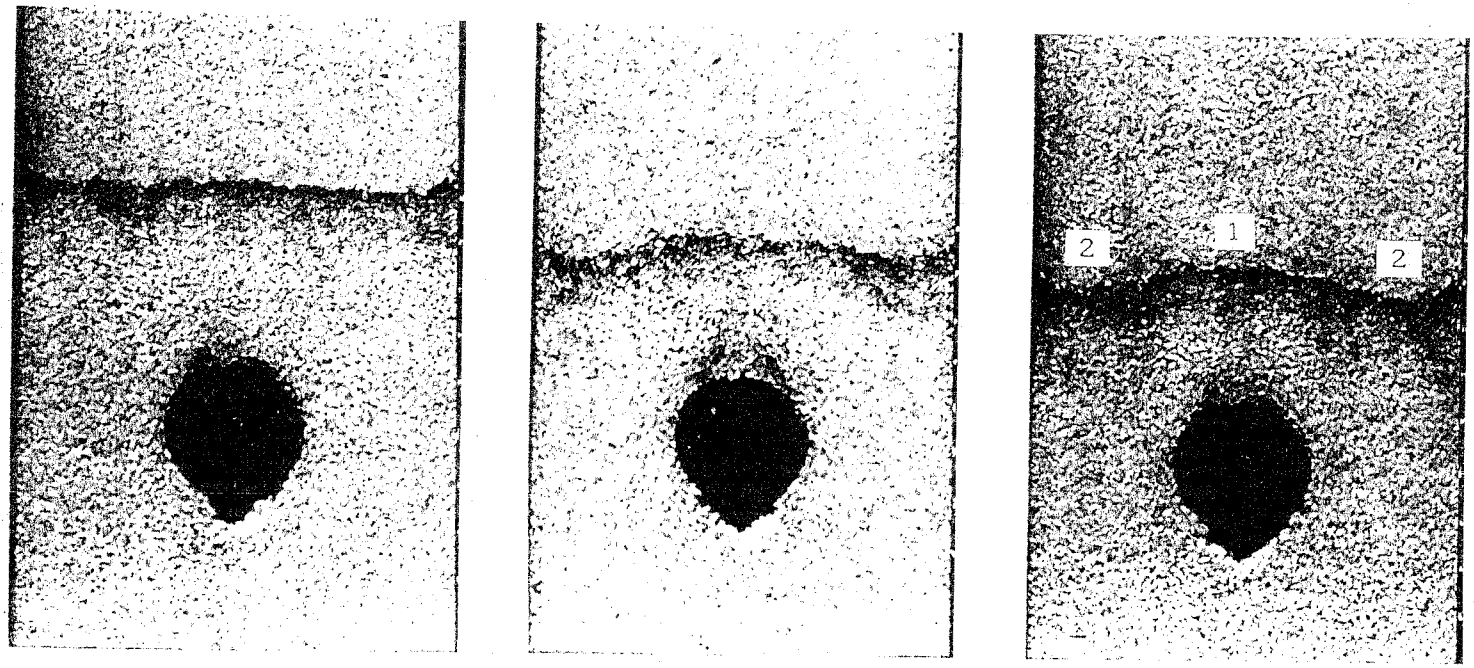

a: x=-1.67 D b: x=-1.33 D c: x=-1.17 D

Fig. 3-a:

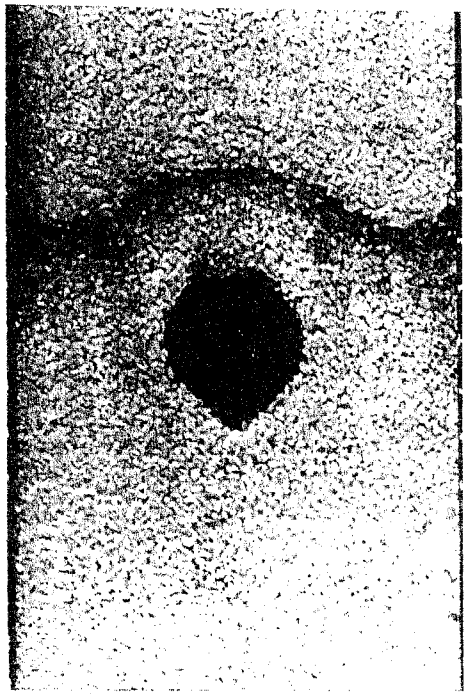

d: x=-0.83 D

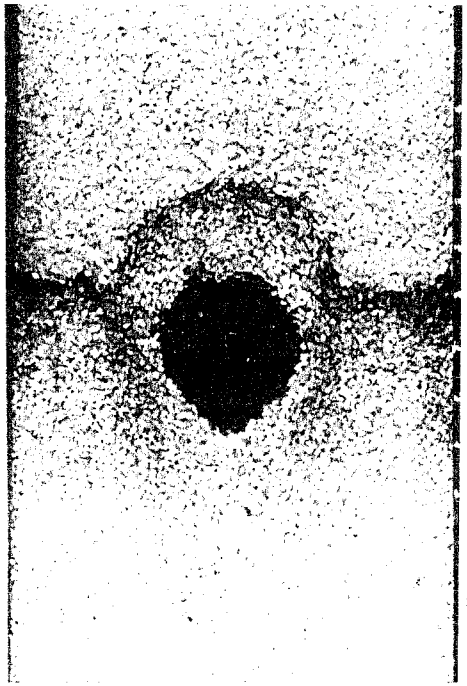

e: x=-0.50 D

f: x/D = 0

Fig. 3-b:

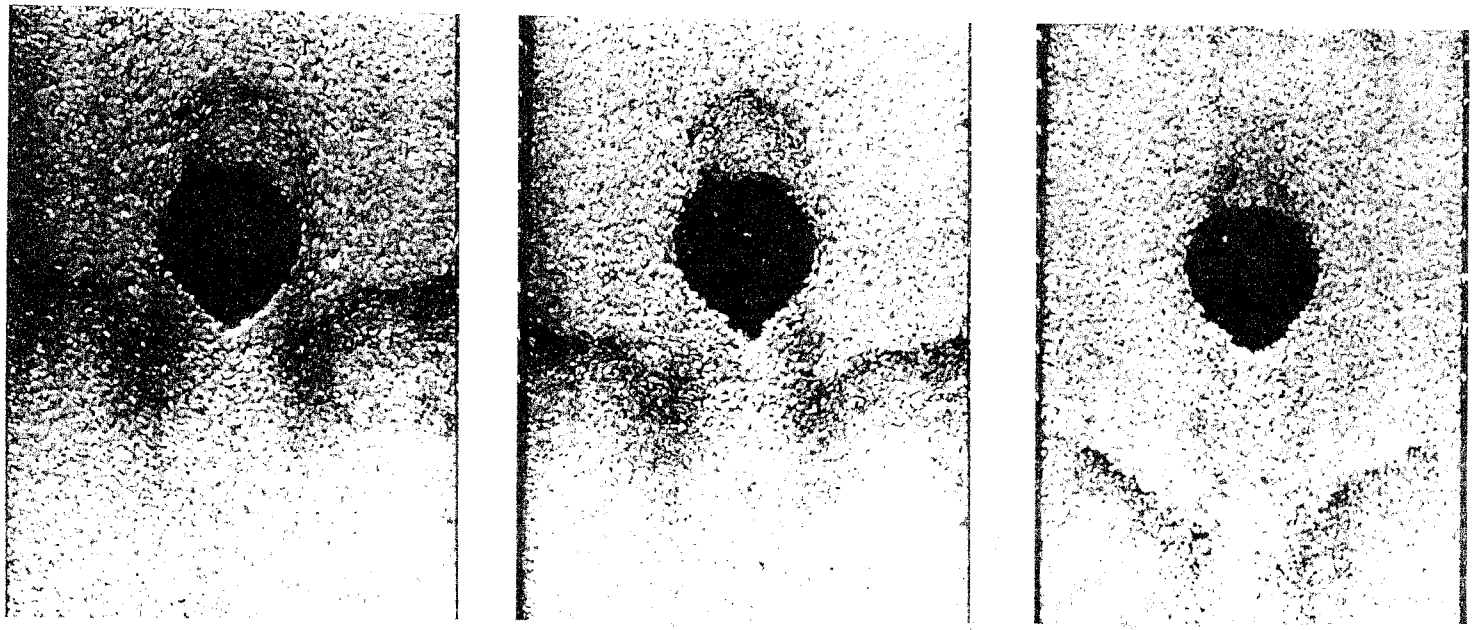

g: x= 0.33 D

h: x= 0.67 D

j: x= D

Fig. 3-c:

Fig. 3-a,b,c: Photographs of development grains flow patterns over cylindrical surfaces at D = 60 mm and V_m = 2 mm/sec.

mm/sec. As can be seen, the following stages could be characterized:

a: Black thin layer at x = 1.67 D from the centerline of the cylinder is not affected by the flow field. The flow separation region could be observed.

b: Small deformation in the black layer at x = 1.33 D and the layers were affected by the cylinder existence.

c: Development of the deformation at x = 1.17 D : Under the effect of the flow, the front part (1) delays and the side parts (2) move downwards into areas of higher flow velocity.

d and e: Continuous deformation of the black layer and hence, the flow pattern could be observed at x = 0.83 D . As could be seen, the flow pattern was greatly affected by the cylinder at x=0.5 D. A stationary layer of particles always exists on the surface of the cylinder.

f: Flow pattern in the vicinity of the cylinder was realized at x/D=0. The thin black layer outer edges reaches the horizontal center line of the cylinder. As a consequence, three main regions are distinguished, namely: stagnant, attachment and flow separation regions. The stagnant and flow separation regions extend from x/D = 0.28 to 1.08 in the upstream of the cylinder and from x/D=0.45 to 0.77 in the downstream of the cylinder, respectively. While the attachment region extends from x/D= 0 to 0.28 in the upstream of the cylinder and in the region of x/D=0 to 0.45 in the downstream of the cylinder.

g: The black thin layer at the rear part of the cylinder still affected by the flow field at x= 0.33 D. The particles near the walls move downwards where the velocity is high.

h: The black thin layer is not affected by the flow field at x=0.67 D. The acceleration of the grain particles is observed as they pass at the rear parts of the cylinder.

j: The black thin layer moves downstream and the effect of the cylinder disappeared at x= D.

The flow pattern obtained in the upstream of the cylinder had a stagnant (dead) region formed on the front part of the cylinder. It is characterized by a stagnant packed layers. The grains tend to decelerate as they pass near this region. Near both sides of the cylinder, attachment region (effective working surface) was observed. This region which extends along the sides of the cylinder includes solid particles in continuous motion. The grain particles tend to accelerate as they pass around the cylinder and also at the rear parts. In the downstream of the cylinder, flow separation region was appeared. This region which is relatively smaller than the stagnant region is formed in the rear part of the cylinder. The region dose not contain any solid particles in direct contact with the lower surface of the cylinder. Hence, it is often called the rear air region as seen in Figs 3-a, b and c.

The above mentioned flow pattern was also observed under the conditions of different layers mean velocity for each tested cylinder. The geometric dimensions L, A_d, Z, A_r of the stagnant and rear air regions were observed to be decreased with increasing the layers mean velocity. These dimensions, however, were observed to be increased with increasing the cylinder diameter. It is found that the stagnant region covers from 14.3 to 34.6% of the cylinder diameter, depending upon the region represents between 45.5 and 59.8 % of the cylinder region represents between 45.5 and 59.8 % of the cylinder surface in the considered ranges of mean velocity and cylinder diameter. The flow separation region fully covers from 13 to 32.8 % of the cylinder surface. In the range of the present experiments, the effect of the side walls on the flow pattern disappears at the mean velocity of 2 mm/sec and the diameter ratio of 0.30, except for the narrow regions near both channel walls as shown in photographs.

3.2. Flow Velocity Distribution:

In figures 4, 5 and 6, the flow velocity distribution around the cylinder is illustrated by using the dimensionless velocity coefficient ψ defined by equation (3). As can be seen, in the range of $\beta = 0^\circ$ to 90°, the velocity coefficient ψ increases at the boundary of the dead zone with the increase of the diameter ratio (D/b) and reaches its maximum value at $\beta = 0^\circ$. At the rear part of the cylinder, in the range of $\beta = 90^\circ$ to 153°, an opposite effect of the diameter ratio was found. The value of ψ decreases with increasing the diameter ratio and reaches its minimum values. This behavior of flow velocity coefficient distribution is attributed to the existence of the stagnant layers formed on the front part of the cylinder which increases with increasing the cylinder diameter. The grain particles tend to decelerate as they pass near this layers then accelerate as they pass around the cylinder and the rear parts. This resulted in a decrease in the layers velocity on the front part of the cylinder and an increase on the sides and rear parts. The increase in the grain velocity reduces the stagnant layers by continuous erosion and, hence the geometric dimensions of the accumulated layers decreases. While at the sides and the rear parts of the cylinder the kinetic energy of the layers becomes high hence, the velocity coefficient decreases. For diameter ratios in the range of D/b=0.05 to 0.1, the grains accelerate to some extend greatly near the rear region of the cylinder (x/D=0-0.5) and then decelerate as they flow to the downstream of the cylinder. The acceleration region spreads into the direction of the main flow. Therefore, the velocity coefficient is lower at these regions than that of the rear part. The decrease of the velocity coefficient may be due to the increase of the layers density in the vicinity of the cylinder.

Figure 7 shows the variation of the velocity coefficient ψ with the diameter ratio (D/b) for three values of layers mean

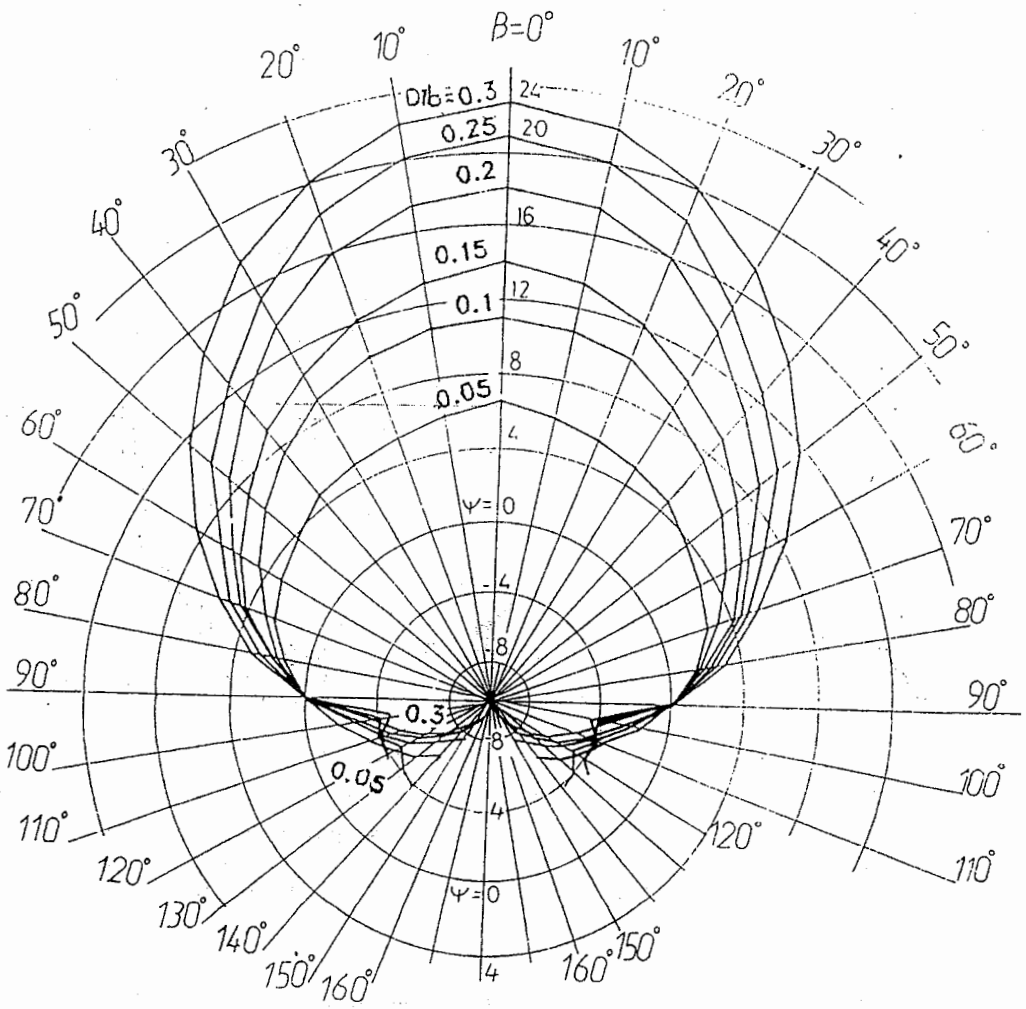

Fig.4 : Flow velocity distribution around the cylinder (V_m = 2 mm/sec.).

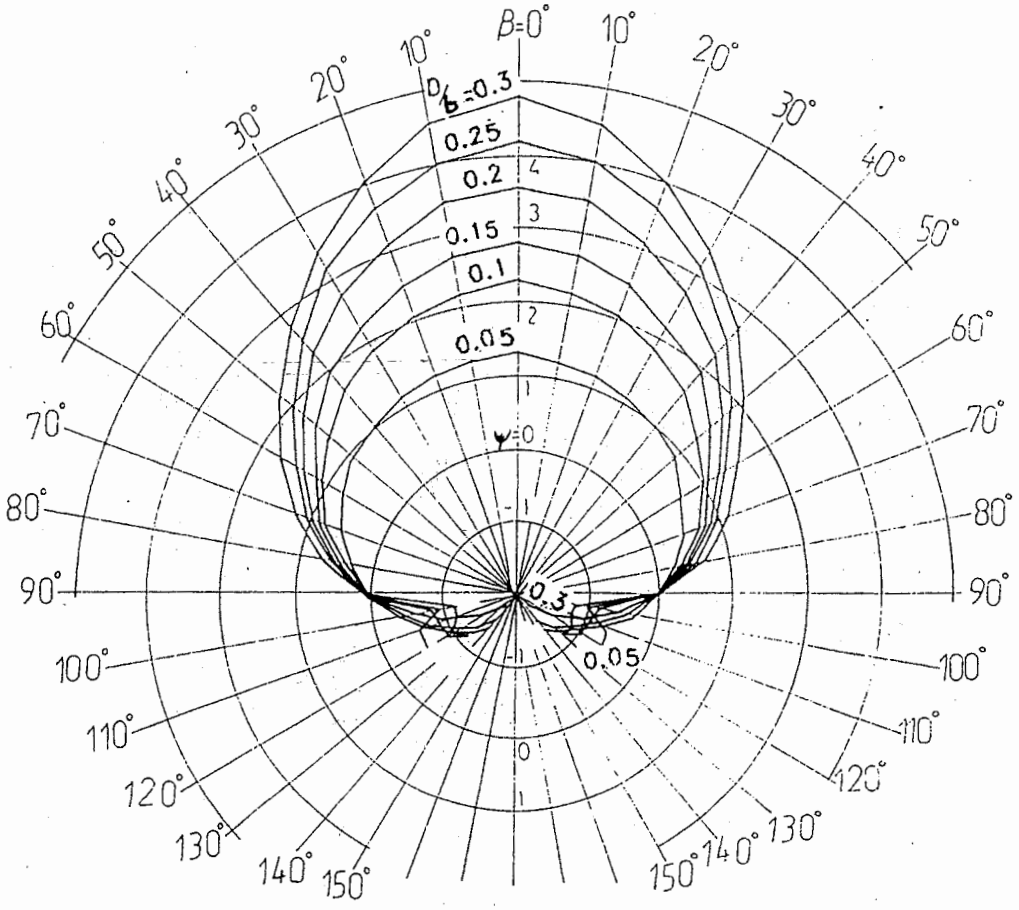

Fig.5 : Flow velocity distribution around the cylinder (V_m = 9 mm/sec.).

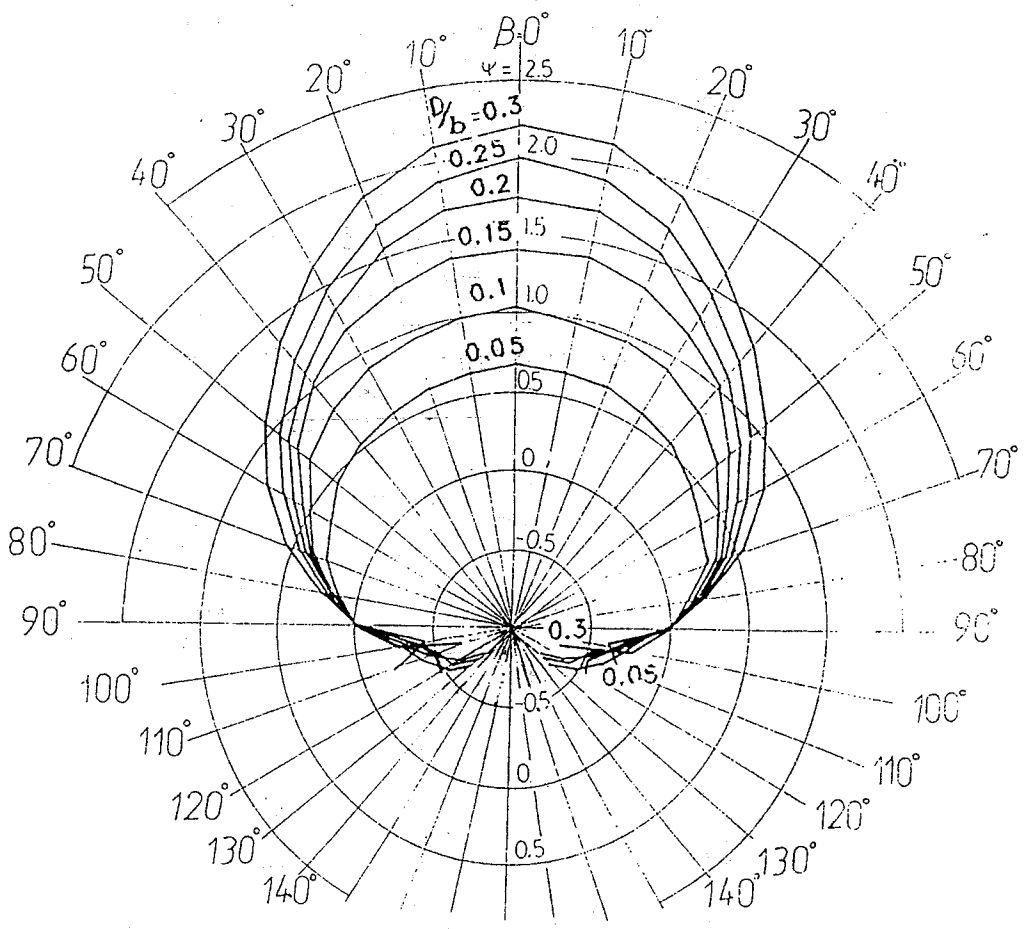

Fig.6 : Flow velocity distribution around the cylinder (V_m = 18 mm/sec.).

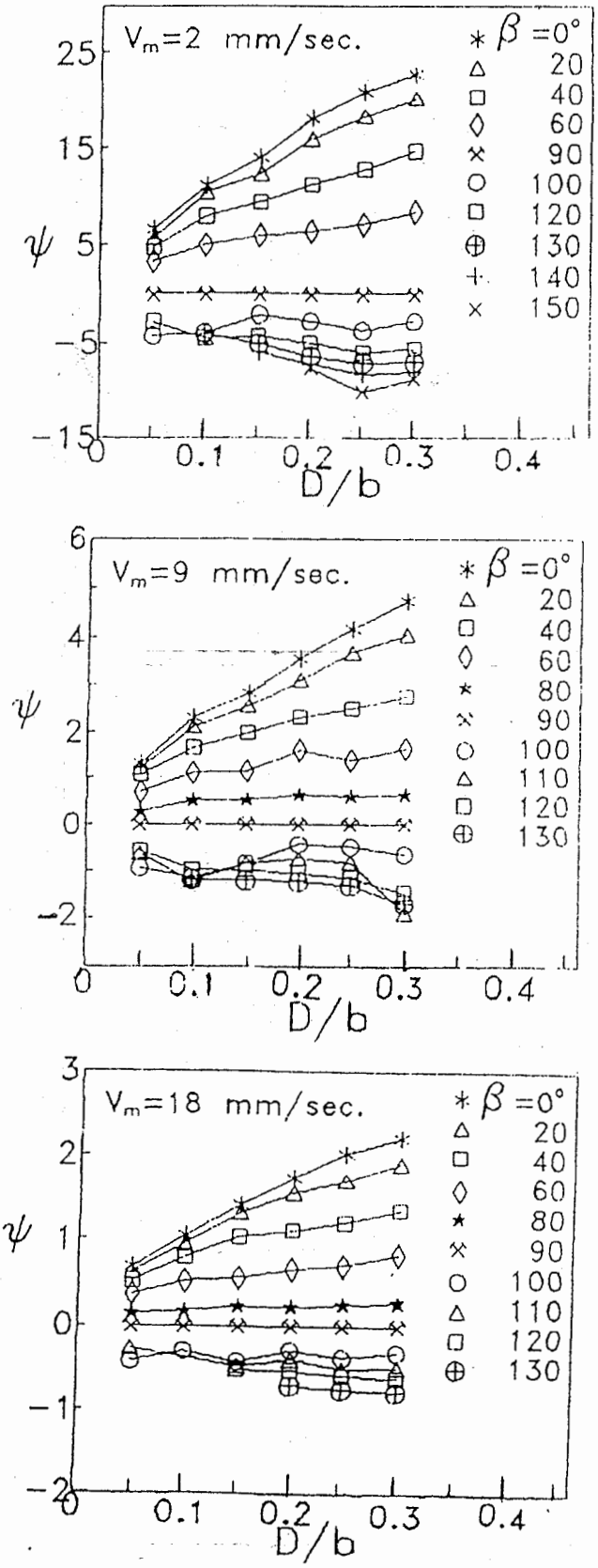

Fig.7 : Variation of flow velocity coefficient ψ with diameter ratio D/b .

velocity V_m = 2, 9 and 18 mm/sec at different angular positions β. The dependence of the velocity coefficient ψ on the layers mean velocity V_m for diameter ratios of 0.05, 0.15 and 0.30 at different angular positions β is also given in Fig. 8. As mentioned before, the increase of the diameter ratio leads to an increase in the stagnant layers on the front part of the cylinder and hence, ψ increases. On the other hand, increasing the particles mean velocity reduces this region and the resistance to the main flow decreases, so ψ decreases. In the rear parts of the cylinder, increasing V_m leads to better mixing of grain layers and results in the decrease of ψ.

Figure 9 shows the distribution of the average flow velocity coefficient $\bar{\psi}$ on Y-axis for layers mean velocities of V_m = 2, 9 and 18 mm/sec at different values of diameter ratios. The variation of the velocity coefficient with the diameter ratio in the upstream and downstream of the cylinder for layers mean velocities of 2, 9 and 18 mm/sec is shown in Fig. 10. The solid lines represent the results for the layers in the upstream, while the dashed lines are for the downstream of the cylinder. From these figures, the following results can be obtained:

1- The average flow velocity coefficient $\bar{\psi}$ first increases with increasing x/D ratio in the upstream of the cylinder up to a certain region of x/D=0.93 to 1.4, depending on the layers mean velocity and the diameter ratio. After that it remains constant. The flow field is not affected by the wake of the cylinder.

2- In the downstream of the cylinder, the increase of $\bar{\psi}$ with increasing x/D extends from 0.73 to 1.15, which also depends on the layers mean velocity and the diameter ratio. The constant values of $\bar{\psi}$ in the upstream and downstream of the cylinder were found to occur according to the range of the diameter ratio and layers mean velocity given in Table 1.

3- In the range of V_m =2-9 mm/sec, $\bar{\psi}$ in the downstream of the cylinder equals to that in the upstream for the region of x/D=0-0.35 . In the downstream of the cylinder $\bar{\psi}$ is larger than that in the upstream for the region of x/D=0.5-1.0. For x/D>1, in the far upstream of the cylinder, $\bar{\psi}$ is independent of x/D ratio.

4- In the range of V_m =14-18 mm/sec, $\bar{\psi}$ in the downstream and upstream of the cylinder is equal for the region of x/D=0-0.5. At x/D=0.75, $\bar{\psi}$ in the downstream is larger than that in the upstream of the cylinder. For x/D > 0.75, $\bar{\psi}$ is not changed with x/D ratio.

5- For all diameter ratios (D/b=0.05-0.30), $\bar{\psi}$ equals zero for x/D=0. At x/D > 0, the increase of $\bar{\psi}$ with increasing the diameter ratio is remarkable.

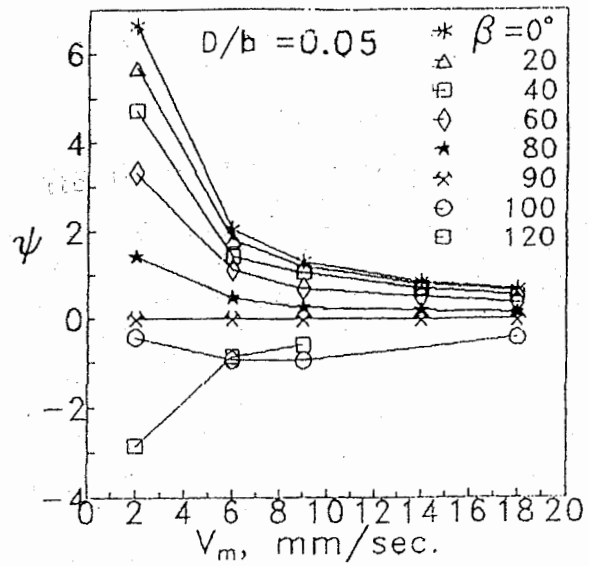

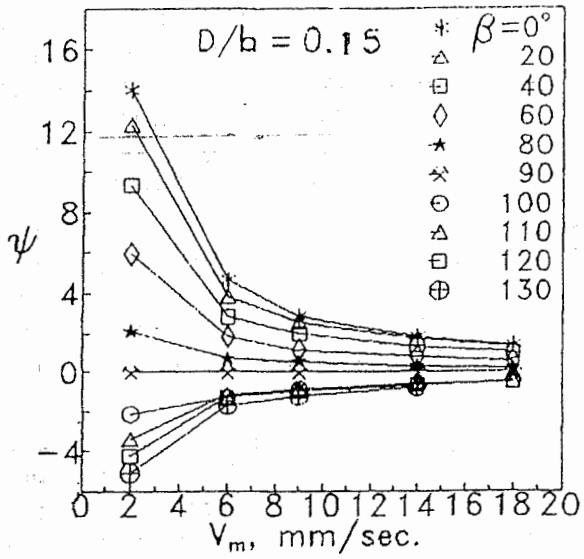

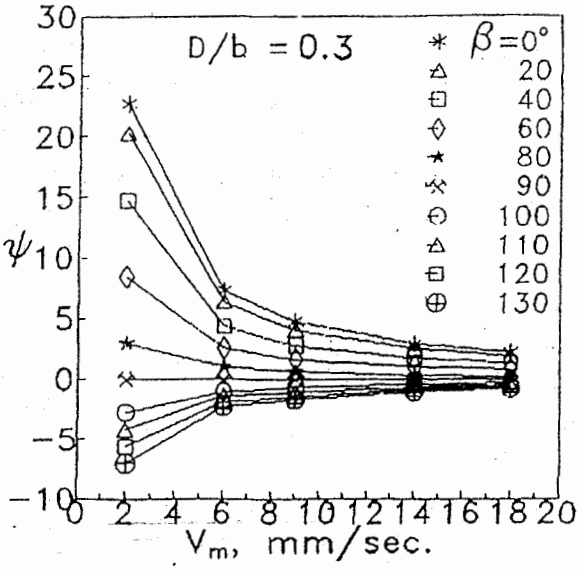

Fig.8 : Variation of flow velocity coefficient ψ with layers mean velocity V_m.

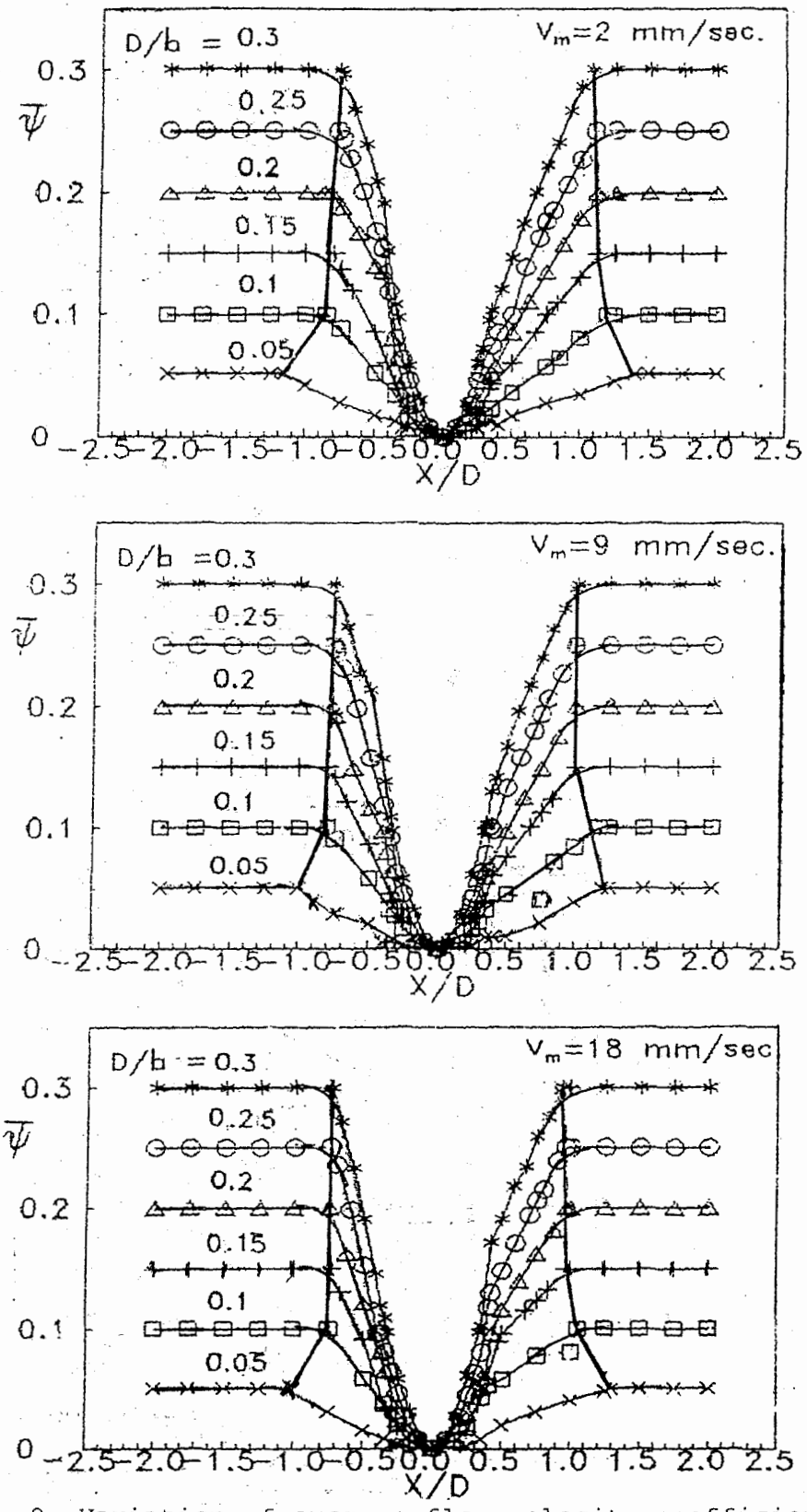

Fig. 9: Variation of average flow velocity coefficient $\bar{\psi}$ on Y-axis in the upstream and downstream of the cylinder

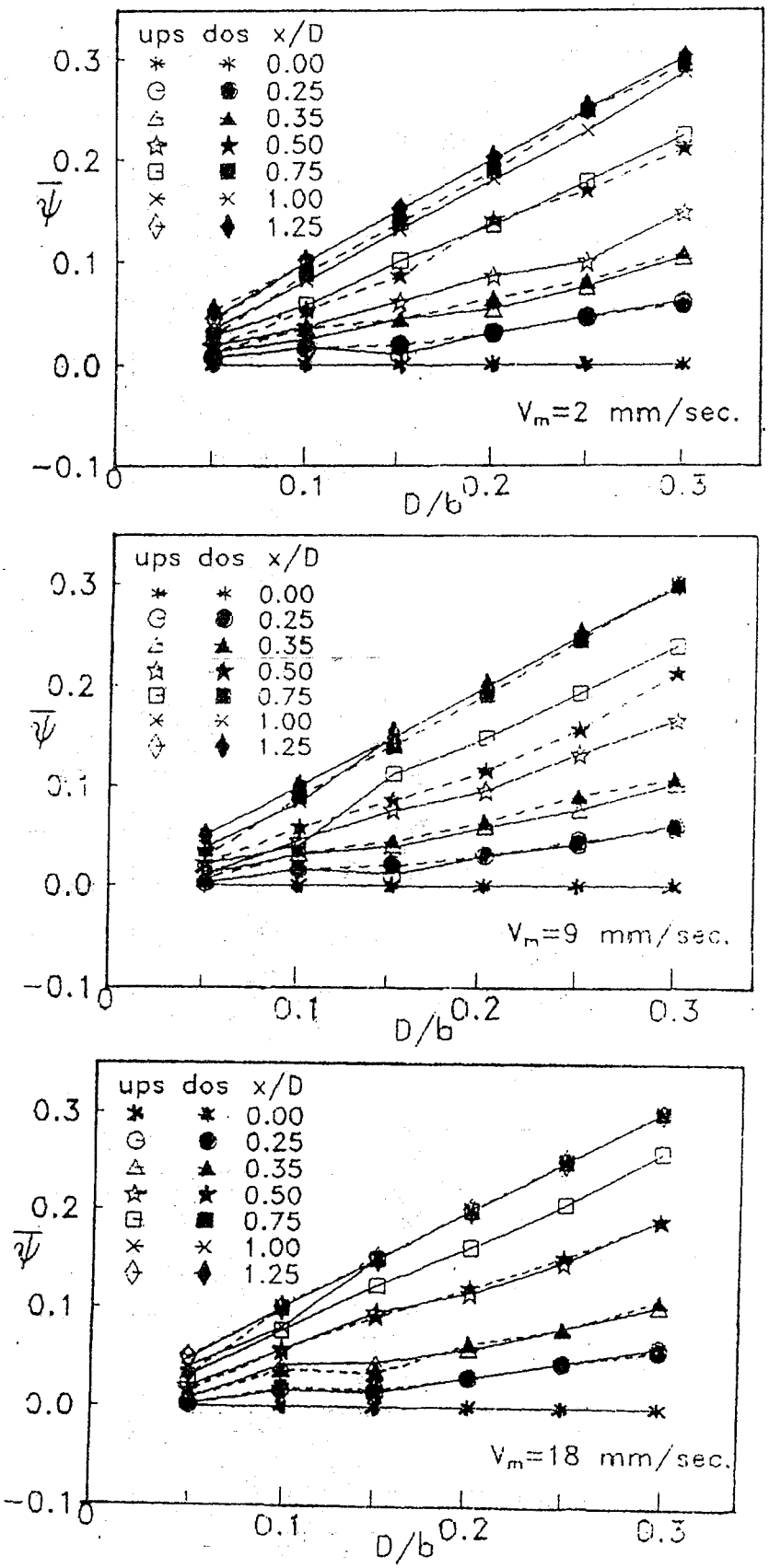

Fig. 10: Variation of average flow velocity coefficient $\bar{\psi}$ with the diameter ratio in the upstream and downstream of the cylinder.

Table 1: Constant flow velocity coefficient range in the upstream and downstream of the cylinder.

Parameter	x/D	D/b	V_m, mm/sec.
Upstream of the cylinder	$1.18 \leq x/D \leq 1.40$	0.05-0.10	2-9
	$1.05 \leq x/D \leq 1.25$	0.05-0.10	14-18
	$1.02 \leq x/D \leq 1.12$	0.15-0.30	$2\text{-}9X_1$
	$0.93 \leq x/D \leq 1.00$	0.15-0.30	14-18
Downstream of the cylinder	$0.80 \leq x/D \leq 1.15$	0.05-0.10	2-9
	$0.75 \leq x/D \leq 1.00$	0.05-0.10	14-18
	$0.75 \leq x/D \leq 0.85$	0.15-0.30	2-9
	$0.73 \leq x/D \leq 0.77$	0.15-0.30	14-18

In the upstream of the cylinder, the increase of $\bar{\psi}$ with the increase of (x/D) ratio is due to a decrease of the local layers velocity which is influenced by the formation of the stagnant region formed in the front part of the cylinder. This results in a decrease of $\bar{\psi}$. At (x/D) greater than 0.93, for example, the effect of the stagnant region disappeared and the front part of the cylinder is more exposed to the main flow. Therefore, the flow velocity coefficient remains constant. In the downstream of the cylinder, the layers velocity is also affected by the existence of the flow separation region formed in the rear part. At (x/D) higher than 0.73 the effect of this region disappears and $\bar{\psi}$ remains constant. The increase in the stagnant and flow separation regions geometric dimensions with increasing cylinder diameter leads to an increase of the ratio (x/D). On the other hand, the dimensions of these regions decrease with increasing the layers mean velocity, which leads to a decrease of (x/D) ratio. The results indicate that the height of the stagnant region represents about 70 to 80 % of the cylinder diameter at the stagnation point $\beta = 0^\circ$ for the diameter D=60 mm, while it reaches 45 to 57% for D=10 mm, depending on the particles mean velocity. The great amount of the accumulated region with respect to the small area of the cylinder (D=10 mm, D/b=0.05) leads to an increase in the dimensionless position (x/D) to 1.4 compared with the other cylinders.

The thick solid line drawn in Fig. 9 represents the line of $(x/D)_{max}$, which reflects the variation of $(x/D)_{max}$ as the diameter ratio (D/b) changed from 0.05 to 0.30. The increase of (D/b) leads to an increase in the maximum velocity coefficient ψ_{max}. However, when the cylinder diameter increases, the density of the deposited stagnant layers increases, Therefore, the flow velocity coefficient and consequently, the maximum flow velocity coefficient increase.

From the present visual observations and the diagrams presented in Figs. 3 to 10, it can be noticed that the stagnant

and flow separation regions occur at all values of the flow conditions. The removal and/or reducing these regions means increasing the effective working surface and hence, the improvement of the drying unit performance. Further experiments and analytical work, however, is still needed in order to overcome these regions. The injection effect of air stream on these regions, for example, may be required to reduce their dimensions. The results are hoped to be useful in the application of heat pipe-heat exchanger systems in the field of drying agriculture products.

4. CONCLUSIONS:

Based on the the experimental results described above, the following conclusions can be obtained:

1. Stagnant, attachment and flow separation regions formed around the cylinder play a significant role in determining the flow pattern in the wake around the cylinder as well as the flow velocity coefficient.
2. Factors affecting the character of the flow velocity coefficient include a strong dependence on both of the grains mean velocity and the diameter ratio. Flow velocity coefficient decreases with increasing the layers mean velocity while it increases with raising the diameter ratio.
3. In the range of angular position between 0° and 90°, the flow velocity coefficient increased over the surface of the cylinder with the increase of the diameter ratio. The maximum value occurs at angular position of 0°. In the range between 90° and 153° in the downstream of the cylinder, the flow velocity coefficient decreases and the minimum values exist.
4. Flow velocity coefficient in the upstream and downstream of the cylinder depends on the dimensionless position (x/D). The velocity coefficient increases with increasing the dimensionless position up to a certain region depending on the layers mean velocity and the diameter ratio. After that it remains constant. The constant region represents the maximum value of the velocity coefficient and its range is presented in Table 1.

NOMENCLATURE:

A_d	Area of the stagnant region, mm^2
A_r	Area of the separation region, mm^2
b	Channel width, mm.
D	Diameter of the test cylinder, mm.
D/b	Diameter ratio.
L	Height of the stagnant region, mm.
V_l	Layers local velocity, mm/sec.
V_{ml}	Layers local mean velocity, mm/sec.

V_m	Layers mean velocity in the main flow, mm/sec.
V_{max}	Layers theoretical velocity at the horizontal centerline of the cylinder, mm/sec.
x	Vertical distance measured from the centerline of the cylinder, mm.
x/D	Dimensionless height ratio.
Z	Depth of the separation region, mm.
β	Angular position, degree.
$\underline{\psi}$	Local flow velocity coefficient.
ψ	Average flow velocity coefficient.
ups.	Upstream of the cylinder.
dos.	Downstream of the cylinder.

REFERENCES:

1- Dunn, P. D. and Reay, D. A., Heat Pipes, Third Edition, Oxford and New York, Pergamon Press, PP. 260-261, 1982.

2- Elson, C. R., The Heat Pipe and Its Possible Applications in the Food Industry. Scientific and Technical Surveys, No. 89, The British Food Manufacturing Industries, Leatherhead, Survey, U. K., 1989.

3- Paikert, P., The Heat Pipe in Heat Recovery, Air Conditioning and Drying, Rev. Prat. Froid Condit. Air, Vol. 30, PP. 35-40, 1977.

4- Pordo, D. G., Krethkee, B. E., Habib, M. A., Heat Transfer in Heat Pipes for Preheating Grains Before Drying, Vcecyou. Naych. Conf., 26-28 May 1987, Moscow, PP. 29-31, 1987.

5- Habib, M. A., The Use of Heat Pipes for Grains Wheat Heat Treatment, Ph. D. Thesis, Odessky Tech. Inst. Peche. Prom., Odessa, 1988.

6- Balanin, B. A.; Acceleration of Solid Particles in a Channel, Eng. Phis. J., Vol. 8, No. 1, PP. 16-20 1990.

7- Zuukauskas, A., and Karni, J., High-Performance Single Phase Heat Exchangers, 2nd.ed., NEW YORK, Hemisphere Publishing Co., PP. 187-192, 1988.

8- Inoue, A., Kozawa, Y., Yokosawa, M. and Aoki, S.; Studies on Two-Phase Cross flow, Part 1: Flow Characteristics Around a Cylinder, In. J. Multi phase Flow, Vol. 12, No. 2, PP. 149 - 167, 1986.

9- Inoue, A., Kozawa, Y., Yokosawa, M. and Aoki, S.; Studies on Two-Phase Cross flow, Part 2: Transition Reynolds Number and Drag Coefficient, In. J. Multi phase Flow, Vol. 12, No. 2, PP. 169-184, 1986.

10-Habib, M. A., and Shams El-Din, SH. H., An Experimental Investigation of Solid Grains Flow Over Cylindrical Surfaces, Jordanian Chemical Eng. Conf. 1, October 18-20, Amman-Jordan, Vol. 1, PP. 126-161, 1993. and in; Eng. Research Bulletin, Faculty of Eng., Menoufiya University, Vol. 19, Part 1, PP. 35-55, 1996.

ملاحظة السريات ومنحنيات السرعة للحبوب المنسابة حول اسطوانـــــة

ملخص البحث :

فى هذا البحث تم ملاحظة نموذج السريان ودراسة شكل منحنيات السرعـــة لحبيبات الارز المنسابة حول الأسطح الاسطوانية ـ تم تصوير تطور نموذج السريان المنساب حول الاسطح الاسطوانية فى المناطق المتأثرة قبل وبعد ـ كما تم ايضا مناقشة تغير معامل سرعة السريان قبل وبعد الاسطوانة وكذلك حول الاسطوانة وتأثير كل من نسبة الأقطار والسرعة المتوسطة للحبوب عليـــه.

تم الحصول على نموذج السريان المنتج حول السطح الاسطوانى عن طريق أسلوب الاثر الاسود حتى يمكن الحصول على معاملات توزيع السرعة ـ تغيرت نسبة الاقطـار من ٠٫٥ الى ٣ ـ وتغيرت سرعة السريان المتوسطة من ٢ الى ١٨مم/ث.

من ملاحظات نموذج السريان ومن تعيين معاملات السرعة لسريان حبوب الارز وجد ان المناطق المتكونة حول السطح الاسطوانى تلعب دورا هاما فى تعيين نموذج السريان حول الاسطوانة وهى تعتمد بشكل كبير على كل من نسبة الاقطار والسرعة المتوسطـــة للحبـــــــوب.